



## Experimental investigation on flame pattern formations of DME–air mixtures in a radial microchannel

Aiwu Fan<sup>a,b,\*</sup>, Kaoru Maruta<sup>b</sup>, Hisashi Nakamura<sup>b</sup>, Sudarshan Kumar<sup>c</sup>, Wei Liu<sup>a</sup>

<sup>a</sup>School of Energy and Power Engineering, Huazhong University of Science and Technology, 1037 Luoyu Road, Wuhan, China

<sup>b</sup>Institute of Fluid Science, Tohoku University, 2-1-1 Katahira, Aoba-ku, Sendai, Japan

<sup>c</sup>Aerospace Engineering Department, IIT Bombay, Powai, Mumbai, India

### ARTICLE INFO

#### Article history:

Received 17 September 2009

Received in revised form 29 April 2010

Accepted 27 May 2010

Available online 19 June 2010

#### Keywords:

DME

Microcombustion

Flame pattern formation

Rotary flame

Oscillating flame

### ABSTRACT

Flame pattern formations of premixed DME–air mixture in a heated radial channel with a gap distance of 2.5 mm were experimentally investigated. The DME–air mixture was introduced into the radial channel through a delivery tube which connected with the center of the top disk. With an image-intensified high-speed video camera, rich flame pattern formations were identified in this configuration. Regime diagram of all these flame patterns was drawn based on the experimental findings in the equivalence ratio range of 0.6–2.0 and inlet velocity range of 1.0–5.0 m/s. Compared with our previous study on premixed methane–air flames, there are several distinct characteristics for the present study. First, Pelton-wheel-like rotary flames and traveling flames with kink-like structures were observed for the first time. Second, in most cases, flames can be stabilized near the inlet port of the channel, exhibiting a conical or cup-like shape, while the conventional circular flame was only observed under limited conditions. Thirdly, an oscillating flame phenomenon occurred under certain conditions. During the oscillation process, a target appearance was seen at some instance. These pattern formation characteristics are considered to be associated with the low-temperature oxidation of DME.

© 2010 The Combustion Institute. Published by Elsevier Inc. All rights reserved.

### 1. Introduction

Power generation by burning hydrocarbons to drive various kinds of Micro-Electro-Mechanical-Systems (MEMS) has received great interest in the past decade. This is mainly due to the much higher energy densities of hydrocarbon fuels as compared with those of the conventional electrochemical batteries [1,2]. However, as the dimension of combustion chamber is reduced, surface area-to-volume ratio increases remarkably which leads to large heat losses [3,4] and radical quenching [4] by the solid walls. Therefore, to sustain a stable flame under reduced scales, thermal management, for instance, heat recirculation, is a frequently adopted strategy for designing miniaturized combustors. The “Swiss Roll” combustor, which was first developed by Lloyd and Weinberg [5], is a typical heat-recirculating-type burner in which fresh mixture is preheated by the hot burned gas through the solid walls. Recently, such structures have been implemented to extend flammability limits of micro- and meso-scale combustors [6–8]. However, flame is usually not observable because of the in-transparent wall of practical combustors. Thus, in the fundamental

studies of microcombustion, some researchers applied straight or radial microchannels made of transparent materials in their experiments to facilitate direct observation of the flame [9–20]. The combustion chamber is optical accessible and thus flame dynamics can be distinguished in detail. To approximately simulate the heat-recirculation effect, Maruta et al. [9,10] used an external heat source to establish a positive wall temperature gradient in the flow direction before the introduction of the fuel. They systematically investigated the combustion characteristics of premixed CH<sub>4</sub>–air mixtures in U-shaped and straight quartz tube of a 2.0-mm diameter. In addition to stable flame, they also observed flame with repetitive extinction and ignition (FREI) and pulsating flame with an image-intensified high-speed video camera. Later, those flame propagation modes were theoretically interpreted by Minaev et al. [11]. Similar flame phenomena were also found experimentally or numerically by other researchers [12–15]. In addition, Xu and Ju [16] and Miesse et al. [17] observed multiple discrete flames in straight and Y-shaped small channels. More recently, through 1D numerical computation, Minaev et al. [18] revealed that flame splitting phenomena exist under certain scenarios in heated microchannels. This was confirmed by the experiments of Fan et al. [19].

Applying the same method as that of Maruta et al. [9,10], Kumar et al. [20–22] and Fan et al. [23–25] performed experimental investigations on flame pattern formations of CH<sub>4</sub>–air mixtures in a heated radial microchannel which can be used as a combustion

\* Corresponding author at: School of Energy and Power Engineering, Huazhong University of Science and Technology, 1037 Luoyu Road, Wuhan 430074, China. Fax: +86 27 87540724.

E-mail address: [faw@mail.hust.edu.cn](mailto:faw@mail.hust.edu.cn) (A. Fan).

chamber in micropower generation devices or systems, such as disk-type microgas turbines [26]. In addition to conventional stable circular flame, a variety of non-stationary flame patterns, such as rotary Pelton-wheel-like flame, spiral-like flame, traveling flame, and so forth, were observed. Regime diagrams of those flame patterns in the radial microchannels with different gap distance were drawn based on systematical experiments, from which it can be clearly seen that flame pattern is a function of the inlet mixture velocity, the mixture equivalence ratio and the channel gap distance [23].

Recently, to reduce environmental pollutions caused by the direct combustion of fossil fuels and to solve the diminishing energy supply, Dimethyl ether (DME), which is considered as a suitable alternative fuel and can be produced from a variety of feedstock, has gained much attention because of its unique chemical properties [27]. Extensive studies on DME performance in Diesel engines have been carried out which demonstrate that DME is a desirable fuel for Diesel engines, due to its high cetane number and volatility that result in short ignition delays, low noise levels and good cold-start characteristics [28]. Meanwhile, DME can reduce NO<sub>x</sub>, HC, and CO emissions, and it does not produce soot [28]. Fischer et al. [29] and Curran et al. [30] developed a detailed kinetic mechanism of DME oxidation including 78 species and 351 reactions. A reduced model was also developed using the CSP method [31], which resulted in 39 species and 168 reactions. The reduced chemistry has very good accuracy for lean flames and has a great advantage in saving computation time. Ignition delay times and OH time-histories in DME oxidation were measured using a shock tube [32]. Extinction limits and flame bifurcation of lean premixed DME–air flames were numerically investigated using the counterflow flame with a reduced chemistry [33]. It was found that the combined effect of radiation and flow stretch led to a new flame bifurcation (high stretch weak flame) and multiple flame regimes. Combustion tests were conducted in a gas turbine by comparing DME with methane, in terms of combustion instability, NO<sub>x</sub> and CO emissions, and the outlet temperature of the combustion chamber [34]. The experiments showed that DME combustion was very clean but hard to control. Moreover, the pressure fluctuation in the combustion chamber caused by combustion instability of DME, was lower than that occasioned by burning methane. It was also ascertained that DME combustion is more likely to flash back than methane combustion [34].

Very recently, ignition and combustion characteristics of a stoichiometric DME–air mixture in a straight micro-tube with a controlled temperature profile were investigated experimentally and numerically by Oshibe et al. [35]. Multi-stage oxidation in low temperature condition was found in their study. Due to the similar wall temperature profile and the unique physiochemical properties of DME, it is expected that particular and complicated features of DME combustion might occur in the heated radial microchannel used in our previous investigations [23–25]. In the present paper, we report the experimental findings of DME flames over a wide equivalence ratio range in a heated radial microchannel. As we have studied the gap distance effect in earlier work [23], and also because all the new findings of DME–air flame patterns could be included in the case with a gap distance of 2.5 mm, other results of different gap distances are not presented in this paper. Special attentions will be paid to the comparisons between flame patterns of DME–air mixtures and those of CH<sub>4</sub>–air mixtures.

## 2. Experimental setup and method

The experimental setup used in the present study is identical to that used in our previous studies [20–25] on premixed CH<sub>4</sub>–air combustion, which is schematically shown in Fig. 1. Two circular

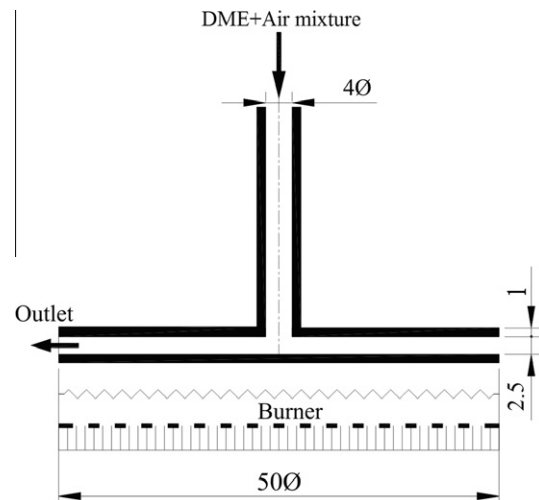


Fig. 1. Schematic diagram of the experimental setup.

quartz plates ( $\varnothing 50$ ) were maintained parallel to each other with a gap distance of 2.5 mm. The bottom plate was heated by a sintered metal burner at a constant heating rate. The top plate was warmed up by the bottom one via radiation and convective heat transfer. Before the introduction of fuel gas, a positive temperature gradient along the radial direction was formed in advance by air-flow. The typical wall temperature profile of the bottom disk was carefully measured with a 250- $\mu\text{m}$  K-type thermocouple at an inlet velocity of 2.0 m/s, as shown in Fig. 2. The head of the thermocouple was bent to keep a good contact with the inner surface of the bottom plate. The movement step of the thermocouple was 1.0 mm, which was controlled by a transverse micrometer. The measured temperatures were corrected for heat losses from the thermocouple bead and the corrected temperatures are accurate to  $\pm 5$  K of the actual value. From Fig. 2, it can be seen that the wall temperature increases with the increase of the radial distance and the maximal value is about 900 K. Also noted is that the temperature gradient in the region of small radius is greater than that in the region of large radius. The mixture delivery tube connected with the top plate and was designed to maintain the upstream temperature of the incoming mixture at  $\sim 300$  K. The flow rate of the supplied fuel–air mixture was monitored through electric mass flow controllers within an accuracy of  $\pm 1\%$ . In order to maintain a rigorous laminar flow in the delivery tube, the maximum value of the inlet velocity was set at 5.0 m/s, where the representative Reynolds number is  $\sim 1280$ . Dimethyl ether (DME) gas at atmo-

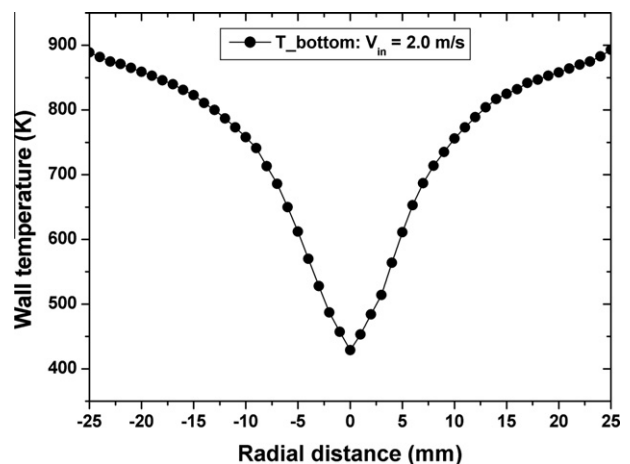


Fig. 2. Measured temperature profile of the bottom plate when  $V_{in} = 2.0$  m/s.

spheric pressure was used as fuel. The flame pattern formations were recorded with an image-intensified high-speed video camera at a rate of 1000 frames per second with a shutter speed of 1/1000 s. Captured images were further analyzed using the software PFV-Ver.2.4.2.0.

### 3. Flame pattern formations

Experimental observations with the image-intensified high-speed video camera showed that rich flame pattern formations (see Figs. 3 and 4) occurred in the heated radial microchannel, in which the circular flame (Fig. 3a), single, double and triple Pelton-wheel-like flames (Fig. 3b–d), traveling flames (Fig. 3g), conical flame (Fig. 3i), cup-like flame (Fig. 3j), and oscillating flame (Fig. 4) were also observed in our previous studies on premixed CH<sub>4</sub>/air flames in the same configuration [20–25]. In addition, single and double Pelton-like flames and traveling flames with kink-like structures (Fig. 3e, f and h) were newly found and reported here for the first time. Regime diagram of those flame patterns is depicted in Fig. 5, in which experiments were conducted under all the conditions denoted by the nodes. The nodes without symbols mean that no flame was observed under those conditions. For the convenience of discussion, inlet mixture velocity in the delivery tube is used as the horizontal axis instead of the mixture flow rate in Fig. 5.

From an overview of Fig. 5 it is seen that the flammable region on the rich side is much larger than that on the lean side. Other researchers also reported that flame speed of DME peaks at an equivalence ratio of  $\sim 1.20$  [36], which is different from that of methane ( $\sim 1.05$ ) [37]. Brief discussions of each flame pattern are given below.

From Fig. 5 it can be seen that at an inlet mixture velocity of 1.0 m/s, a conical flame (see Fig. 3i) locating at the inlet port was observed in the equivalence ratio range of 1.05–1.50. Under conditions which are denoted by the red triangle symbols, the flame exhibits a cup-like shape stabilizing near the inlet port (see Fig. 3j). This flame shape is a deformation of the lengthened conical flame due to the constraint of the narrow gap distance between the two disks. Comparing Fig. 5 with the regime diagrams of CH<sub>4</sub>-air flames of our previous study [23], it is shown that the conical and cup-like flames of CH<sub>4</sub>-air mixtures only occurred under low inlet velocity conditions, i.e., 1.0 m/s and 1.5 m/s. However, for the case of DME-air mixtures, the conical and cup-like flames can be stabilized near the inlet port up to an inlet velocity of 4.0 m/s. In other words, the region occupied by the conical and cup-like flames of DME-air mixtures is much wider than that of CH<sub>4</sub>-air mixtures. Lee et al. reported that flashback was more likely to take place for DME than CH<sub>4</sub> in a gas turbine [34]. However, the reasons for their case are considered to be different from ours. In their case, the inlet temperature was much higher and most of the flashbacks were affected by mixing and ignition characteristics. For example, Chen et al. [38] showed that the ignition delays of DME-air mixtures were much shorter than those of CH<sub>4</sub>-air mixtures. In the present work, the higher flame speed of DME as compared with CH<sub>4</sub> was the main cause of the increased flame stabilization range [36].

Under the conditions represented by the blue circles in Fig. 5, flame has a circular front. The radial location of the circular flame depends on both the inlet mixture velocity and the mixture equivalence ratio. The region occupied by the circular flame is relatively narrow as compared with that by the cup-like and conical flames which could be considered as a limit of the circular flame.

Near the flammability limits at moderate inlet velocity, one, two or even three discrete Pelton-wheel-like flames rotating around the central axis at a frequency of  $\sim 20$ –55 Hz appear in the radial channel. The rotation frequency is a function of the mixture equivalence ratio and the inlet velocity. The rotating

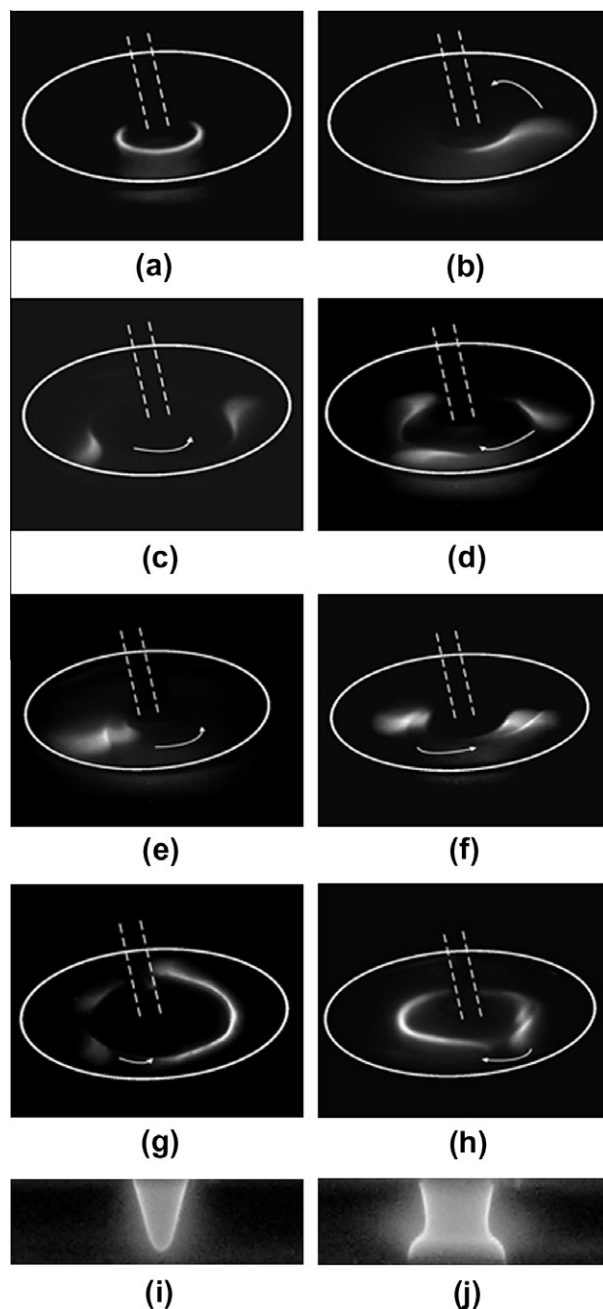


**Fig. 3.** One frame of different flame patterns observed in the radial microchannel: (a) circular flame at  $V_{in} = 3.0$  m/s and  $\phi = 0.95$ , (b) single Pelton-wheel-like flame at  $V_{in} = 2.5$  m/s and  $\phi = 0.75$ , (c) double Pelton-wheel-like flame at  $V_{in} = 3.0$  m/s and  $\phi = 1.85$ , (d) triple Pelton-wheel-like flame at  $V_{in} = 4.0$  m/s and  $\phi = 1.80$ , (e) single Pelton-wheel-like flame with kink-like structures at  $V_{in} = 3.0$  m/s and  $\phi = 1.65$ , (f) double Pelton-wheel-like flame with kink-like structures at  $V_{in} = 3.5$  m/s and  $\phi = 1.70$ , (g) traveling flame at  $V_{in} = 4.0$  m/s and  $\phi = 0.65$ , and (h) traveling flame with kink-like structures at  $V_{in} = 5.0$  m/s and  $\phi = 0.70$ , (i) conical flame at  $V_{in} = 1.0$  m/s and  $\phi = 1.3$  (side view), (j) cup-like flame at  $V_{in} = 2.0$  m/s and  $\phi = 1.2$  (side view). Here  $V_{in}$  and  $\phi$  are the inlet mixture velocity and equivalence ratio, respectively. Fig. 3a–h were captured by a high-speed digital video camera, while Fig. 3i and j were taken by a common digital still camera. Solid and dashed white lines indicate the position of the top plate and mixture delivery tube, respectively. Arrows are drawn to indicate the rotating direction of the rotary flame patterns.

direction and the number of the Pelton-wheel-like small flames have random possibilities, which manifest the bifurcation characteristics of flame pattern formations for the near-limit mixtures. For slightly leaner and richer mixtures than those near the flammability limits on both the rich and lean sides, the Pelton-wheel-like

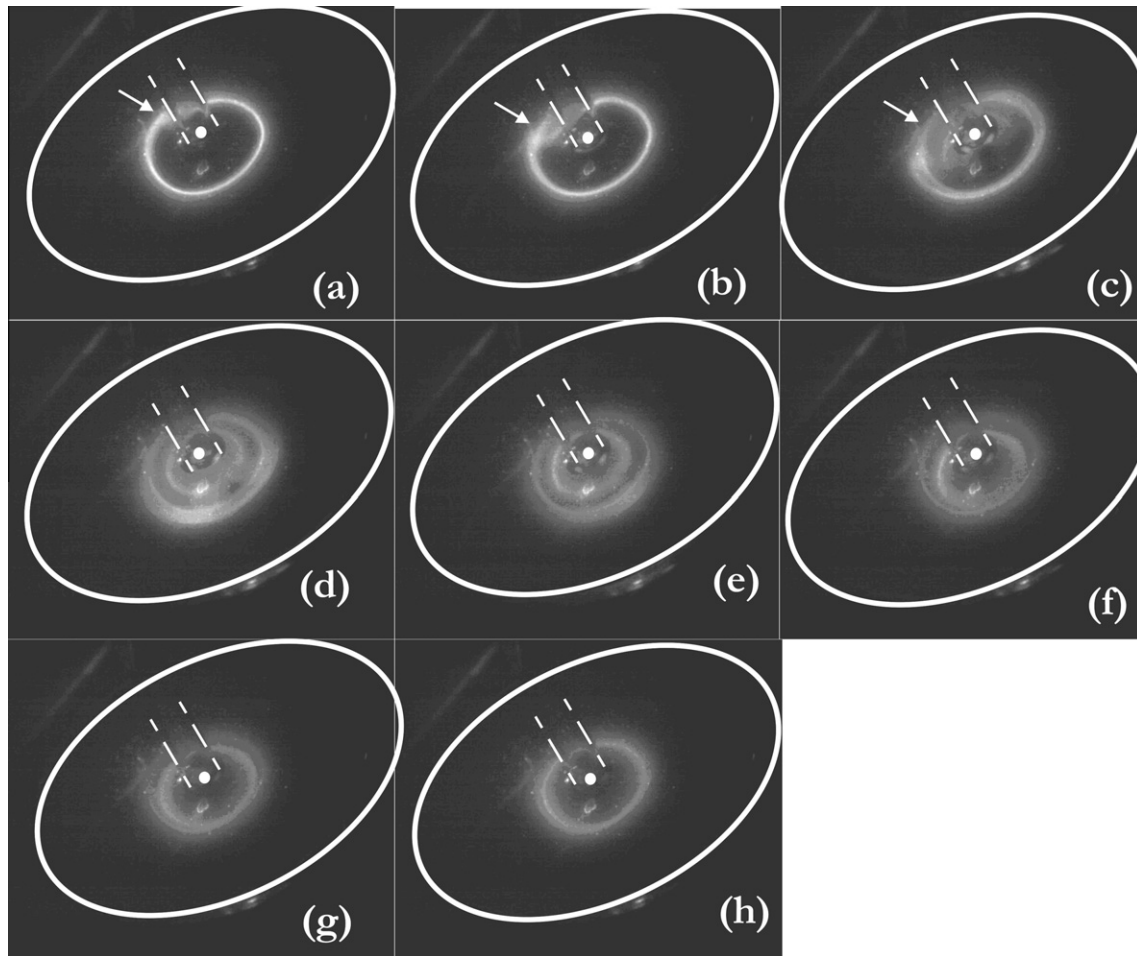


Fig. 4. Eight sequential frames of the dynamic process of an oscillating flame at  $V_{in} = 3.5$  m/s and  $\phi = 1.10$ .

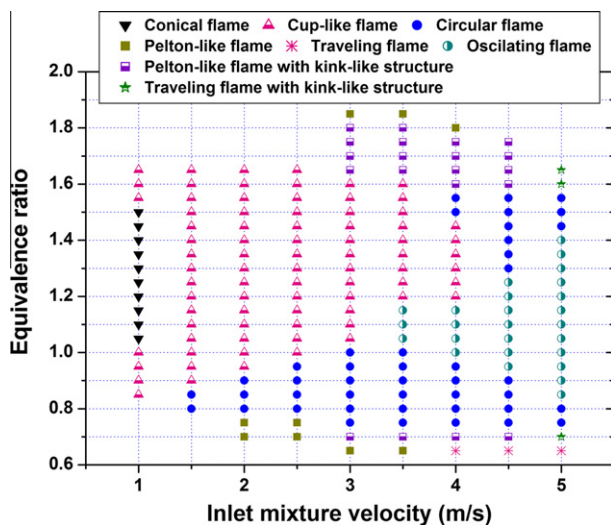


Fig. 5. Flame pattern regime diagram of DME-air mixtures.

flames exhibit appearances with kink-like structures, as shown in Fig. 3e and f. The same phenomenon was also observed in the traveling flame (see Fig. 3h). To help examining those new flame patterns in details, we take the single Pelton-wheel-like flame with kink-like structures as an example and six sequential frames of its evolution process were presented in Fig. 6. Although the exact

mechanism still remains unclear at the present stage, we consider it might be associated with the low temperature oxidization of DME because the wall temperature is relatively low at the location of the inner part of the flame front. Further discussions about this will be given in Section 4.

Fig. 4a–h shows the evolution of an oscillating flame. At the first stage, flame splitting, which was recently reported by Minaev et al. [18] and Fan et al. [19], occurs at some location (indicated by the white arrow in Fig. 4a) and subsequently it develops into a flame kink as seen in Fig. 4b and c. Then, the unburned mixture in close vicinity to the flame kink is ignited and a circular flame with a smaller radius forms. This can be clearly seen from Fig. 4d and e which shows two circular flame fronts coexist at different radial locations. Alternate layers of fresh reactants and combustion products exist at the interfaces for a very short time. Due to adverse conditions of high mixture velocity and low residence time, the inner flame front moves outwards. The original flame front at a larger radius weakens with time due to unavailability of fresh reactants and finally disappears. The outward movement of inner flame and simultaneous disappearance of original flame are shown in Fig. 4e–h. Although the oscillating flame dynamics was also observed in premixed  $\text{CH}_4$ -air flames [39], it occurred more frequently in the present investigation of DME-air mixtures.

#### 4. Discussions

Looking at the photos of all those flame patterns and their distribution in the regime diagram, one can imagine that all the non-

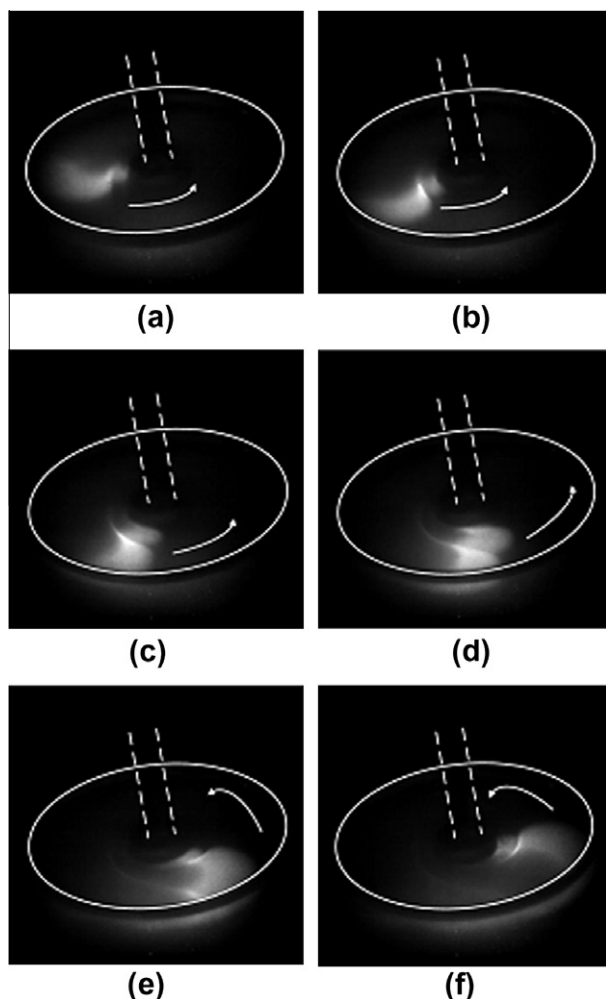


**Fig. 6.** Six sequential frames of the rotating process of the single Pelton-wheel-like flame with kink-like structures at  $V_{in} = 4.0$  m/s and  $\phi = 1.70$ .

stationary flames originate from the circular flame. The change of the flame shape is due to the local flame blowout. In the present configuration, a positive temperature gradient and a negative flow velocity coexist in the radial direction. At the meantime, the mixture flow is a jet into a confined space formed by the channel walls. Due to the sudden change in flow direction, detachment and reattachment of the mixture flow occur near the wall surfaces at different radial locations. In addition, there exist a temperature difference between the bottom and upper disks (maximal value  $\sim 30$ – $50$  K), which may probably lead to a buoyancy-induced instability. Thus, onset of flame instability can have many sources, such as thermo-diffusive instability, hydrodynamic instability, buoyancy-induced instability, or a coupling of some/all of them. For example, in our previous paper [25], the Pelton-wheel-like flame was successfully re-produced using a 2D thermo-diffusive model without considering momentum transport and temperature gradient in the vertical direction. However, other rotary flames cannot be numerically realized using the same model. This shows that other instabilities might also play important roles in the formations of other flame patterns. Three dimensional model considering heat and momentum transports, detailed chemistry, as well as buoyancy effect might be the best selection in future simulations.

As for the newly observed kink-like structures, although the mechanisms still remain unclear, it is expected that low-temperature oxidation may be the most probable reason. It is well known that DME has rich low temperature chemistry. In the present

investigation, the wall temperature range up to 900 K is the right window for low temperature combustion of DME. Very recently, low-temperature oxidations of stoichiometric DME–air mixture were carefully examined in a microflow-reactor by Oshibe et al. [35]. They found two- and even three-stage low-temperature oxidations through experiments and 1D numerical simulation with detailed chemistry. The similarity between their study and the present work is that controlled wall temperature profiles were adopted in both cases. Thus, some underlying physics of flame pattern formations should be similar in those two cases. But the situations are more complicated in the case of the heated radial microchannel than the counterparts of the straight micro-tube.

Another fact that shows the consistency in flame pattern formation mechanisms is the flame splitting phenomenon. Minaev et al. reported that flame splitting phenomenon existed in both the heated straight micro-tube and radial microchannel through 1D numerical simulations [18]. Later, Fan et al. confirmed this phenomenon via experiments in the heated micro-tube [19]. As mentioned in Section 3 of this paper, the oscillating flame mode was also originated from local splitting of the circular flame front, although the dynamic process was more complicated than that in the straight tube.

## 5. Concluding remarks

We reported flame pattern formations of DME–air mixtures in a heated radial microchannel with a gap distance of 2.5 mm. A variety of flames termed conical flame, cup-like flame, circular flame, Pelton-wheel-like flame and traveling flame with and without kink-like structures, and oscillating flame were observed. Regime diagram of all those flame patterns has been obtained and presented. Comparing the present work with our previous study of premixed  $\text{CH}_4$ –air flames, some distinct characteristics of DME combustion were found in the heated radial microchannel.

- (1) Pelton-wheel-like flame and traveling flame with kink-like structures were observed and reported here for the first time. These flame structures are considered to be related with the low-temperature oxidations of DME.
- (2) In the flame pattern regime diagram, the flammable region on the rich side is much larger than that on the lean side.
- (3) Flame is prone to be stabilized near the inlet port of the radial microchannel, exhibiting conical or cup-like shapes, which demonstrates that premixed DME–air flame is easier to flash back than the premixed methane–air flame in the same configuration.
- (4) An oscillating flame frequently occurs at relatively high inlet velocities for mixtures with a moderate equivalence ratio.

To fully reveal the underlying mechanisms of those flame pattern formations, theoretical and numerical investigations are in progress in our group, although it is a tough and time-consuming task. New results on this subject will be reported in our future paper.

## Acknowledgments

The authors would like to thank Mr. S. Hasegawa and Mr. T. Tezuka for their assistance in conducting the present experiments. This work was supported by the Natural Science Foundation of Hubei Province, China (20092020), and partially supported by the Foundation of State Key Laboratory of Coal Combustion, China (FSKLCC0816) and the Foundation of Huazhong University of Science and Technology, China (M2009007).

## References

- [1] A.C. Fernandez-Pello, Proc. Combust. Inst. 29 (2002) 883–899.
- [2] J. Vican, B.F. Gajdeczko, F.L. Dryer, D.L. Milius, I.A. Aksay, R.A. Yetter, Proc. Combust. Inst. 29 (2002) 909–916.
- [3] T.T. Leach, C.P. Cadou, Proc. Combust. Inst. 30 (2005) 2437–2444.
- [4] S. Raimondeau, D. Norton, D.G. Vlachos, R.I. Masel, Proc. Combust. Inst. 29 (2002) 901–907.
- [5] S.A. Lloyd, F.J. Weinberg, Nature 251 (1974) 47–50.
- [6] F.J. Weinberg, P.D. Ronney, Proc. Combust. Inst. 29 (2002) 941–947.
- [7] C.H. Kuo, P.D. Ronney, Proc. Combust. Inst. 31 (2007) 3277–3284.
- [8] N.I. Kim, S. Kato, T. Kataoka, T. Yokomori, S. Maruyama, T. Fujimori, K. Maruta, Combust. Flame 141 (2005) 229–240.
- [9] K. Maruta, J.K. Parc, K.C. Oh, T. Fujimori, S.S. Minaev, R.V. Fursenko, Combust. Explos. Shock Waves 40 (2004) 516–523.
- [10] K. Maruta, T. Kataoka, N.I. Kim, S. Minaev, R. Fursenko, Proc. Combust. Inst. 30 (2005) 2429–2436.
- [11] S. Minaev, K. Maruta, R. Fursenko, Combust. Theory Model. 11 (2007) 187–203.
- [12] F. Richecoeur, D.C. Kyritsis, Proc. Combust. Inst. 30 (2005) 2419–2427.
- [13] Y. Fan, Y. Suzuki, N. Kasagi, Proc. Combust. Inst. 32 (2009) 3083–3090.
- [14] T.L. Jackson, J. Buckmaster, Z. Lu, D.C. Kyritsis, L. Massa, Proc. Combust. Inst. 31 (2007) 955–962.
- [15] G. Pizza, C.E. Frouzakis, J. Mantzaras, A.G. Tomboulides, K. Boulouchos, Combust. Flame 152 (2007) 433–450.
- [16] B. Xu, Y.G. Ju, Proc. 5th US Combustion Meeting, San Diego, USA, 2007.
- [17] C.M. Miesse, R.I. Masel, M. Short, M.A. Shannon, Proc. Combust. Inst. 30 (2005) 2499–2507.
- [18] S.S. Minaev, E.V. Sereshchenko, R.V. Fursenko, A. Fan, K. Maruta, Combust. Explos. Shock Waves 45 (2009) 119–125.
- [19] A.W. Fan, S.S. Minaev, E.V. Sereshchenko, Y. Tsuboi, H. Oshibe, H. Nakamura, K. Maruta, Combust. Explos. Shock Waves 45 (2009) 245–250.
- [20] S. Kumar, K. Maruta, S.S. Minaev, Phys. Rev. E 75 (2007) 016208.
- [21] S. Kumar, K. Maruta, S.S. Minaev, Proc. Combust. Inst. 31 (2007) 3261–3268.
- [22] S. Kumar, K. Maruta, S.S. Minaev, J. Micromech. Microeng. 17 (2007) 900–908.
- [23] A.W. Fan, S.S. Minaev, S. Kumar, W. Liu, K. Maruta, Combust. Flame 153 (2008) 479–489.
- [24] A.W. Fan, S.S. Minaev, S. Kumar, W. Liu, K. Maruta, J. Micromech. Microeng. 17 (2007) 2398–2406.
- [25] A.W. Fan, S.S. Minaev, E.V. Sereshchenko, R.V. Fursenko, S. Kumar, W. Liu, K. Maruta, Proc. Combust. Inst. 32 (2009) 3059–3066.
- [26] C.M. Spadaccini, A. Mehra, J. Lee, X. Zhang, S. Lukachko, I. Waitz, J. Eng. Gas Turbines Power 125 (2003) 709–719.
- [27] C. Arcoumanis, C. Bae, R. Crookes, E. Kinoshita, Fuel 87 (2008) 1014–1030.
- [28] G. Fast, D. Kuhn, A.G. Class, U. Maas, Combust. Flame 156 (2009) 200–213.
- [29] S.L. Fischer, F.L. Dryer, H.J. Curran, Int. J. Chem. Kinet. 32 (2000) 713–740.
- [30] H.J. Curran, S.L. Fischer, F.L. Dryer, Int. J. Chem. Kinet. 32 (2000) 741–759.
- [31] T. Lu, Y. Ju, C.K. Law, Combust. Flame 126 (2001) 1445–1455.
- [32] R.D. Cook, D.F. Davidson, R.K. Hanson, Proc. Combust. Inst. 32 (2009) 189–196.
- [33] Y. Ju, Y. Xue, Proc. Combust. Inst. 30 (2005) 295–301.
- [34] M.C. Lee, S.B. Seo, J.H. Chung, Y.J. Joo, D.H. Ahn, Fuel 87 (2008) 2162–2167.
- [35] H. Oshibe, H. Nakamura, T. Tezuka, S. Hasegawa, K. Maruta, Combust. Flame (2010), doi:10.1016/j.combustflame.2010.03.004.
- [36] X. Qin, Y. Ju, Proc. Combust. Inst. 30 (2005) 233–240.
- [37] S.R. Turns, An Introduction to Combustion, second ed., McGraw-Hill, New York, 2000, pp. 278–279.
- [38] Z. Chen, X. Qin, Y. Ju, Z. Zhao, M. Chaos, F.L. Dryer, Proc. Combust. Inst. 31 (2007) 1215–1222.
- [39] S. Kumar, K. Maruta, S.S. Minaev, Phys. Fluids 20 (2008) 024101.